General Disclaimer

One or more of the Following Statements may affect this Document

- This document has been reproduced from the best copy furnished by the organizational source. It is being released in the interest of making available as much information as possible.

- This document may contain data, which exceeds the sheet parameters. It was furnished in this condition by the organizational source and is the best copy available.

- This document may contain tone-on-tone or color graphs, charts and/or pictures, which have been reproduced in black and white.

- This document is paginated as submitted by the original source.

- Portions of this document are not fully legible due to the historical nature of some of the material. However, it is the best reproduction available from the original submission.

Produced by the NASA Center for Aerospace Information (CASI)

COLLISIONAL DAMPING OF SURFACE WAVES

IN THE SOLAR CORONA

Bruce E. Gordon

and

Joseph V. Hollweg

.

Space Science Center
Department of Physics
University of New Hampshire
Durham, NH 03824

June 1982

ABSTRACT

It has been suggested that surface waves may be able to heat the solar corona. These waves can propagate into the corona and supply the required energies, and because they are linearly compressive they can be dissipated by ion viscosity and electron heat conduction. In this paper we evaluate the damping of surface waves by viscosity and heat conduction. For the solar corona, it is found that surface waves dissipate efficiently only if their periods are shorter than a few tens of seconds and only if the background magnetic field is less than about 10 Gauss. Heating of quiet coronal regions is possible if the coronal waves have short periods, but they cannot heat regions of strong magnetic field, such as coronal active region loops.

I. Introduction

The mechanisms which convert the kinetic energy of the solar photosphere
and convection zone into the thermal energy of the corona have been under
investigation for some four decades. In spite of intensive and imaginative
effort, no successful theoretical solution to the coronal heating problem
has been offered (see recent reviews by Chiuderi, 1979; Hollweg, 1981a;
Kuperus, Ionson and Spicer, 1981; Wentzel, 1981; Withbroe, 1981).

Coronal heating by MHD waves has been widely investigated. The MHD
slow mode can probably be ignored in this context, since it propagates too
slowly to carry the required energy flux into the corona, subject to the
constraints imposed by the observed amplitudes of non-thermal motions in
the corona and underlying chromsphere (e.g. Athay and White, 1979a, b; Bruner,
1978; Bruner and Poletto, 1981).

The MHD Alfvén mode has been investigated in this context for many
years (e.g. Alfvén, 1947; Osterbrock, 1961; Piddington, 1956). Even though
't is strongly reflected by the chromosphere corona transition region, the
Alfvén mode does seem capable of carrying the required energy flux into the
corona from below, at least if the wave frequency is not too low (e.g.
Hollweg, 1981b; Hollweg, Jackson, and Galloway, 1982; Leer, Holzer and Fla,
1982; Zugzda and Locans, 1982). The constraints are more severe in active
regions, but Hollweg (1981) and Zugzda and Locans (1982) have shown that
energy can enter coronal active region loops if appropriate resonances in
the coronal active region loops are excited. The effect is similar to anti-
reflectance coatings on camera lenses; Ionson (   ) has discussed it in terms
of resonant LRC circuits. The difficulty with the Alfvén mode is the

dissipation mechanism. Alfven waves are noncompressive (to lowest order), and they therefore do not couple to the radiation field, nor are they damped to any significant extent by viscosity or heat conduction. Alfvén waves are expected to be only weakly nonlinear in the corona, and nonlinear mechanisms are probably inadequate (e.g. Chin and Wentzel, 1972; Uchida and Kaburaki, 1974). A possible exception to this statement has been pointed out by Hollweg, Jackson and Galloway (1982), who noted that Alfvén waves with periods shorter than a few minutes can steepen into shocks in the chromosphere, which subsequently enter the corona from below. Hollweg (1982a) has shown that the shocks can in principle dissipate rapidly enough to heat coronal holes or quiet coronal regions, but the mechanism fails on coronal active region loops.

The MHD fast mode has a number of appealing features. Its group velocity is large and it is therefore in principle capable of carrying a large energy flux in the corona. It is intrinsically compressive, and therefore subject to dissipation by viscosity, heat conduction and radiation, or by Landau and transit-time damping in the high-frequency limit where Coulomb collisions are ineffective. Habbal, Leer, and Holzer (1979) have pointed out that re-fraction can focus the wave energy into selected sites in the corona, thus offering a natural explanation of the observed "structuring" of the corona. However, Habbal, Leer and Holzer simply postulate the existence of an appro-priate flux of fast waves at the coronal base. This approach may not be justified. Osterbrock (1961) has pointed out that fast waves should undergo severe refraction in the chromosphere, where the Alfvén speed increases

rapidly with height; the refraction turns the energy flux away from the corona. In a similar vein, Hollweg (1978) has pointed out that the known solar motions should lead primarily to fast waves which are evanescent in the corona. These conclusions have recently been put on firmer ground by Leroy and Schwartz (1982) and Schwartz and Leroy (1982), who have investigated the behavior of fast waves in a model solar atmosphere which includes the chromosphere, transition region, and corona; they conclude that fast waves can not supply the required energy flux into the corona.

A remaining possibility takes advantage of observations that the corona is highly structured. It is possible that the structuring occurs in the form of very thin tangential discontinuities. Such structures would have thicknesses of only a few proton gyro-radii, which would be totally unresolved in any optical observations of the corona. However, it is worth noting that such tangential discontinuities are very abundant in the solar wind (e.g. Burlaga, 1971; Neubauer and Barnstorf, 1981), occurring as frequently as 1 hour^{-1}; if the solar wind can be used as a guide, the corona may contain tangential discontinuities (TD's). It has been pointed out that TD's can support MHD surface waves (e.g. Edwin and Roberts, 1982; Ionson, 1978; Roberts, 1981a, b; Wentzel, 1979). These waves have properties which may make them capable of heating the corona. They resemble Alfvén waves. Thus, to the extent that Alfvén waves are capable of supplying the required energies to the corona, we surmise that surface waves will be capable of doing so also. But, unlike the Alfvén mode, the surface waves are intrinsically compressive, even in a linearized small amplitude analysis. As pointed out by Hollweg (1981a), this means that the surface waves can be dissipated by viscosity, heat conduction, and radiation, or by Landau and transit-time damping in a collisionless situation.

In this paper we evaluate the extent to which surface waves can be collisionally dissipated in the corona, i.e. we evaluate their dissipation by viscosity, heat conduction and radiation. (Collisional electrical resistivity can safely be neglected in the corona.) Since we are considering collisional dissipation, we will confine our attention to dense coronal regions, where collisions are frequent; coronal holes will be excluded from our analysis. For the simple cases considered, we conclude that the surface waves dissipate in a resonable distance only if their periods are less than a few tens of seconds, and only if the magnetic field strength is less than about 10 Gauss. The collisional damping of surface waves may conceivably serve to heat quiet coronal regions, if the wave periods are short enough. But the large magnetic field strengths which are presumed to exist in coronal active region loops imply that the collisional dissipation of surface waves is too weak to heat those regions.

It should be noted that we are not considering surface wave dissipation by resonance absorption (Ionson, 1978; Lee, 1980; Ral and Roberts, 1982; Lee, Rae, and Roberts, 1982). Resonance absorption may play a role in heating the corona, but we will formally exclude it from our present analysis by considering only true tangential discontinuities, of zero thickness. If resonance absorption does occur, it will represent an extra dissipation mechanism, in addition to the collisional mechanisms being evaluated here.

II. Basic Equations

The dissipation of surface waves in the corona is analysed subject to a number of simplifying assumptions:

1. Gravity is ignored.

2. The magnetic field pressure in the corona is assumed to dominate the thermal pressure. We will therefore ignore the effects of thermal pressure on the lowest-order dynamic properties of the surface waves, i.e. we employ the cold plasma approximation to calculate the properties of the surface waves in the absence of dissipation.

3. The surface waves are assumed to be weakly dissipative in the sense of $k_i/k_z \ll 1$, where k_i is the imaginary part of the wave number and k_z is the real part of the wavenumber component along the background magnetic field, $\underset{\sim}{B}_o$. This permits an approximate procedure for calculating k_i, as follows: The wave properties are first calculated in the absence of dissipation. Then, given those wave properties it is possible to calculate the volumetric rate at which the waves lose energy to radiation, and to heat via viscosity and heat conduction. Finally, the damping length (or k_i) is determined by equating the volumetric energy loss rate to the divergence of the surface wave Poynting flux. This procedure obviates the need to calculate a full wave dispersion relation in the presence of viscosity, heat conduction, and radiation, but it is limited to the weak damping limit. Details of the procedure are given in Section V.

4. The surface wave properties are calculated via small-amplitude linearized theory.

5. Consistent with the cold plasma approximation, the background magnetic field is taken to be uniform, and in the z-direction. The magnetic

field direction does not change across a TD (c.f. Hollweg, 1982b).

6. The background density is assumed to vary only in the x-direction. Thus we will be considering planar discontinuities. Moreover, we shall specialize to two specific cases: i. a single TD which separates two regions of differing density; ii. two parallel TD's which enclose a region where the density differs from that external to the TD's.

7. The background flow velocity is assumed to be zero.

Our analysis is similar to that of Edwin and Roberts (1982), Hollweg (1982b), Roberts (1981a,b), and Wentzel (1979). For clarity and complete-ness, some of our analysis of the wave properties in the absence of dissipation will overlap these previous works, but we consider some new features as well.

In the absence of dissipation, the linearized MHD induction equation is

$$\frac{\partial \delta \underline{B}}{\partial t} = \nabla \times (\delta \underline{v} \times \underline{B}_o) \tag{1}$$

where $\underline{B}$ and $\underline{v}$ denote magnetic field and velocity, the prefix 'δ' denotes a fluctuating wave quantity, and the subscript 'o' denotes the temporally steady background. The linearized momentum equation is

$$\rho_o \frac{\partial \delta \underline{v}}{\partial t} = - \nabla \delta P + \frac{B_{oz}}{4\pi} \frac{\partial \delta \underline{B}}{\partial z} \tag{2}$$

where ρ denotes mass density, and δP is the magnetic pressure fluctuation,

$$\delta P = \underline{B}_o \cdot \delta \underline{B}/4\pi \tag{3}$$

Equation (2) has utilized the fact that $\underline{B}_o$ is constant and in the z- direction. Equations (1) and (3) combine to yield

$$\frac{\partial \delta P}{\partial t} = - \frac{B_o^2}{4\pi} \left(\frac{\partial \delta v_x}{\partial x} + \frac{\partial \delta v_y}{\partial y} \right) \tag{4a}$$

We will find that $\delta v_z = 0$ for the problem at hand, and thus (4a) becomes

$$\frac{\partial \delta P}{\partial t} = -\frac{B_0^2}{4\pi} \, \nabla \cdot \delta \underset{\sim}{v} \tag{4b}$$

We next differentiate (2) with respect to time. The quantities $\delta \underset{\sim}{B}$ and δP can then be eliminated with the aid of (1) and (4b). In virtue of assumption (6), the resulting differential equation for $\delta \underset{\sim}{v}$ has coefficients which are independent of y, z and t. We Fourier analyse in those variables, with solutions of the following form:

$$\delta v_x = +\delta V_{kx}(x) \cos (k_y y) \exp (ik_z z - i\omega t) \tag{5a}$$

$$\delta v_y = -\delta V_{ky}(x) \sin (k_y y) \exp (ik_z z - i\omega t) \tag{5b}$$

$$\delta v_z = +\delta V_{kz}(x) \cos (k_y y) \exp (ik_z z - i\omega t) \tag{5c}$$

where k_y, k_z, and ω are constants. If these equations are inserted into the differential equation for $\delta \underset{\sim}{v}$, we obtain

$$\epsilon \, \delta V_{kx} = k_y \, B_0^2 \, \frac{\partial \delta V_{ky}}{\partial x} - B_0^2 \, \frac{\partial^2 \delta V_{kx}}{\partial x^2} \tag{6}$$

$$q^2 \delta V_{ky} = k_y \, \frac{\partial \delta V_{kx}}{\partial x} \tag{7}$$

$$\delta V_{kz} = 0 \tag{8}$$

The following quantities have been defined:

$$\varepsilon(x) = 4\pi\rho_0(x)\omega^2 - k_z^2 B_0^2 \tag{9}$$

$$q^2 = k_y^2 - \varepsilon/B_0^2 \tag{10a}$$

$$= k^2 - \omega^2/v_A^2 \tag{10b}$$

$$k^2 = k_y^2 + k_z^2 \tag{11}$$

$$v_A^2 = B_0^2/4\pi\rho_0 \tag{12}$$

Equations (6) and (7) combine into the fundamental equation of this paper:

$$\frac{\partial}{\partial x}\left[\frac{\varepsilon}{q^2}\frac{\partial \delta V_{kx}}{\partial x}\right] - \varepsilon\delta V_{kx} = 0 \tag{13}$$

Equation (13) is a special case of similar equations which have appeared previously (Edwin and Roberts, 1982; Hollweg, 1982b; Ionson, 1978; Roberts 1981a,b; Wentzel, 1979).

Up to now $\rho_0(x)$ is an arbitrary function. We now specialize to cases where $\rho_0(x)$ is constant except at the TD's, where $\rho_0(x)$ jumps discontinuously. At a discontinuity, equation (13) must be solved subject to the following jump conditions:

$$\delta V_{kx} = \text{constant} \tag{14a}$$

$$\frac{\varepsilon}{q^2}\frac{\partial \delta V_{kx}}{\partial x} = \text{constant} \tag{14b}$$

Equation (14a) permits both sides of the discontinuity to move together, while (14b) can be obtained by integrating (13) across the discontinuity.

III. The Single TD

Consider the case where $\rho_0 = \rho_{01}$ for $x<0$, and $\rho_0 = \rho_{02}$ for $x>0$, where ρ_{01} and ρ_{02} are constants. We seek surface wave solutions of the form

$$\delta V_{kx1} = A \exp(+|q_1|x), \quad x<0 \tag{15a}$$

$$\delta V_{kx2} = A \exp(-|q_2|x), \quad x>0 \tag{15b}$$

The subscripts '1' and '2' denote $x<0$ and $x>0$, respectively. It has been assumed that $q_1^2>0$ and $q_2^2>0$ (see below). The quantity A is an arbitrary constant. Inserting equations (15) into (14b) yields the dispersion relation:

$$\frac{\epsilon_1}{|q_1|} = -\frac{\epsilon_2}{|q_2|} \tag{16}$$

squaring both sides of (16) and using equations (10) yields

$$(\epsilon_1-\epsilon_2)\left[k_y^2 B_0^2 (\epsilon_1+\epsilon_2) - \epsilon_1\epsilon_2\right] = 0 \tag{17}$$

Consider first the root $\epsilon_1 = \epsilon_2$. This requires that either $\rho_{01} = \rho_{02}$ or $\omega^2 = 0$. The former case eliminates the discontinuity and thus the surface wave, while the latter case merely corresponds to a new steady state. This then leaves the following for the surface wave dispersion relation:

$$k_y^2 B_0^2 = \frac{\epsilon_1\epsilon_2}{\epsilon_1+\epsilon_2} \tag{18}$$

Defining new variables $X \equiv k_z^2 v_{A1}^2$, $Y \equiv \omega^2$, $Z = k_y^2 v_{A1}^2$, equation (18) takes the form

$$Z = \frac{(Y-X)(\beta Y-X)}{(\beta+1)Y-2X} \tag{19}$$

where $\beta \equiv \rho_{0_2}/\rho_{0_1}$. In (19) we will regard β and Z as given, so that Y can be determined as a function of X. Without loss of generality we assume $0 \leq \beta < 1$, and we confine our attention to the first quadrant of the X-Y plane. From (19) it is easily shown that Z is positive only above the line $Y = X/\beta$, or between the lines $Y = X$ and $Y = 2X/(1+\beta)$; since Z is positive definite by assumption, allowed solutions are restricted to tnese two regions. However, valid surface wave solutions require $q_1^2 \geq 0$ and $q_2^2 \geq 0$. By combining equations (10) and (19), it can be shown that these conditions are satisfied only below the line $Y = 2X/(1+\beta)$, and thus valid surface wave solutions arc confined to the second of the two regions specified above. (It is easily shown that ϵ_1 and ϵ_2 have opposite signs in this region, as required by (16). Thus restricting our attention to this region eliminates the extraneous root which was introduced when (16) was squared.)

By examining the discriminant (e.g. Thomas, 1960, Section 9-10) of (19), it is easily shown that (19) generates hyperbolas. Only the branch lying between the lines $Y = X$ and $Y = 2X/(1+\beta)$ need be considered, for the reasons given in the preceding paragraph. This bra..:h has the asymptote

$$Y \to X+Z \tag{20}$$

and it passes through the origin with a slope $2/(1+\beta)$. The phase velocity, ω/k_z, is therefore $\left[2/(1+\beta)\right]^{\frac{1}{2}} v_{A1}$ for low-frequency waves satisfying $\omega^2 << Z/(1+\beta)$, and asymptotically approaches v_{A1} at high-frequencies.

IV. The Slab of Plasma

Consider two TD's located at $x = -a$ and $x = +a$. Let $\rho_0 = \rho_{01}$ for $|x| > a$, and $\rho_0 = \rho_{02}$ for $|x| < a$, where ρ_{01} and ρ_{02} are constants. The subscripts '1' and '2' will refer to $|x| > a$ and $|x| < a$, respectively. We consider only solutions which are localized to the vicinity of the TD's. We therefore assume $q_1^2 > 0$, and look for solutions to (13) of the form

$$\delta V_{kx} = A_1 \exp(-|q_1|x), \quad x > a \tag{21a}$$

$$\delta V_{kx} = \pm A_1 \exp(+|q_1|x), \quad x < -a \tag{21b}$$

Here A_1 is an arbitrary constant, and the $\pm$ in (21b) allows for an arbitrary choice of parity.

The quantity q_2^2 can now be positive or negative. If $q_2^2 > 0$, equation (13) has the following two solutions in region 2 which we distinguish with the labels 'Case I' and 'Case II':

$$\delta V_{kx2} = A_2 \sinh|q_2|x, \quad \text{Case I} \tag{22}$$

$$\delta V_{kx2} = A_2 \cosh|q_2|x, \quad \text{Case II} \tag{23}$$

On the other hand, if $q_2^2 < 0$, equation (13) has solutions (Cases III and IV).

$$\delta V_{kx2} = A_2 \sin|q_2|x, \quad \text{Case III} \tag{24}$$

$$\delta V_{kx2} = A_2 \cos|q_2|x, \quad \text{Case IV} \tag{25}$$

Here A_2 is a constant which in each case is related to A_1 by applying (14a) at $x = a$ or at $x = -a$. (Note that Cases I and III have odd parity, so that

the minus sign must be chosen in (21b). Cases II and IV require the plus sign in (21b).)

The dispersion relation is obtained by applying (14b) at $x = a$ or at $x = -a$. For the four cases defined by equations (22) - (25), we have the following dispersion relations:

Case I: $\quad \xi = -\coth (|q_2|a)$ (26)

Case II: $\quad \xi = -\tanh (|q_2|a)$ (27)

Case III: $\xi = \cot (|q_2|a)$ (28)

Case IV: $\quad \xi = -\tan (|q_2|a)$ (29)

where

$$\xi \equiv \frac{\epsilon_1}{\epsilon_2} \frac{|q_2|}{|q_1|} \quad .$$

Note that equations (26) and (27) reduce to the dispersion relation for a single discontinuity (equation 16) in the limit $a \to \infty$, which is expected since the two TD's do not interact with one another in that limit.

Figures 1a - d plot $\omega^2 a^2/v_{A_2}^2$ vs. $k_z^2 a^2$ for $k_y a = 2$ and $\rho_{o1}/\rho_{o2} = 0.25$. The figures are generated as follows: The quantities $k_y a$ and ρ_{o1}/ρ_{o2} are first chosen. The quantity $|q_2|a$ is then allowed to vary, so that each value of $|q_2|a$ yields one point in Figures 1 a-d. For each value of $|q_2|a$, the quantities $\epsilon_2 a^2/B_o^2$ and ξ can be calculated via equations (10a) and (26) - (29), respectively. From the definition of ξ, it is then possible to determine the value of $(\epsilon_1 a^2/B_o^2) (|q_1|a)^{-1}$. Writing $\epsilon_1 a^2/B_o^2$ in terms of $|q_1|^2 a^2$ via equation (10a) then yields a quadratic equation for $|q_1|^2 a^2$. We solve this equation for $|q_1|a$, and $\epsilon_1 a^2/B_o^2$ is then determined via (10a). Finally, equation (9) is then used to determine

$$\frac{\omega^2 a^2}{v_{A2}^2} = (1 - \frac{\rho_{o1}}{\rho_{o2}})^{-1} (\frac{\epsilon_2 a^2}{B_o^2} - \frac{\epsilon_1 a^2}{B_o^2}) \tag{30}$$

and

$$k_z^2 a^2 = \frac{\omega^2 a^2}{v_{A2}^2} - \frac{\epsilon_2 a^2}{B_o^2} . \tag{31}$$

Several features of the solutions are worth noting:

1. For Cases I and II, we obtain $\omega^2 > 0$ and $k_z^2 > 0$ for $|q_2| < (\cdot) k_y$, if $\rho_{o1} < (>) \rho_{o2}$.

2. For Cases I and II, $\omega^2 \to 0$ and $k_z^2 \to 0$ as $|q_2| \to k_y$. In this limit, it is readily shown that

$$\omega^2 \approx \frac{k_z^2 v_{A2}^2 [1 + \coth(k_y a)]}{(\rho_{o1}/\rho_{o2}) + \coth(k_y a)} \tag{32}$$

for Case I. (For Case II, the coth in (32) must be replaced with tanh.)

3. For Case I with $\rho_{o1} < \rho_{o2}$, $\omega^2 \to \infty$ and $k_z^2 \to \infty$ as $|q_2| \to 0$. In this limit

$$\frac{\omega^2 a^2}{v_{A2}^2} \approx k_z^2 a^2 + k_y^2 a^2 \tag{33}$$

(see equations (31) and (10a)).

4. For Case II with $\rho_{o1} < \rho_{o2}$, ω^2 and k_z^2 approach maximum values as $|q_2| \to 0$. This maximum value is evident in Figure 1b. It is readily shown that these maximum values are

$$\omega_{max}^2 = k_y^2 v_{A2}^2 \frac{1 + (k_y a)^2 \left[1 + (1 + 4k_y^{-2} a^{-2})^{1/2}\right]/2}{1 - (\rho_{o1}/\rho_{o2})} \tag{34}$$

$$k_{z,max}^2 = k_y^2 \frac{(\rho_{o1}/\rho_{o2}) + (k_y a)^2 \left[1 + (1 + 4k_y^{-2} a^{-2})^{1/2}\right]/2}{1 - (\rho_{o1}/\rho_{o2})} \tag{35}$$

5. Cases III and IV exist only when $\rho_{o1} < \rho_{o2}$. Then $v_{A2} < v_{A1}$, and the region between the two TD's can act as a waveguide for the fast MHD mode, with total internal reflection occuring at the TD's. Strictly speaking, Cases III and IV are not true surface waves, but trapped body waves (Edwin and Roberts, 1982). We include Cases III and IV for completeness.

6. The point indicated by the arrow in Figure 1d (Case IV) is for $|q_2|=0$. It is identical to the maximum values of ω and k_z found for Case II (equations 34 and 35).

7. For Cases III and IV, equations (28) and (29) show that $\xi \to +\infty$ for certain values of $|q_2|a$. For these values of $|q_2|a$, it is easily shown that

$$\frac{\omega^2 a^2}{v_{A2}^2} = \frac{|q_2|^2 a^2}{1-(\rho_{o1}/\rho_{o2})} \tag{36}$$

and

$$k_z^2 a^2 = \frac{(\rho_{o1}/\rho_{o2})|q_2|^2 a^2}{1-(\rho_{o1}/\rho_{o2})} - k_y^2 a^2 \tag{37}$$

Some of these points are indicated by the x's in Figures 1c and 1d (there are some additional points with $k_z^2<0$, in virtue of equation 37, which are not shown in the figures).

8. For Cases III and IV, equations (28) and (29) show that $\xi \to -\infty$ for certain values of $|q_2|a$. For these values of $|q_2|a$, it is easily shown that $\omega^2 \to \infty$ and $k_z^2 \to \infty$, with

$$\frac{\omega^2 a^2}{v_{A2}^2} \sim k_z^2 a^2 + k_y^2 a^2 + |q_2|^2 a^2 \tag{38}$$

asymptotically (see equations 31 and 10a).

V. Collisional Dissipation.

As discussed in the Introduction, we wish to calculate the dissipation of the surface waves by viscosity, heat conduction, and radiation. We will do the calculation for the plasma slab (see Section IV); the case of a single discontinuity can then be obtained by letting a → ∞.

The volumetric heating rate due to viscosity, Q_{vis}, is given by Braginskii (1965, equation 2.28):

$$Q_{vis} = \frac{\eta_o}{3} (\nabla \cdot \delta \underset{\sim}{v})^2 \tag{39}$$

where it is assumed that $\delta v_z = 0$ and that the ions undergo many cyclotron orbits between collisions. The viscosity is due mainly to the protons. From Braginskii's equations (2.5i) and (2.22) we have

$$\eta_o = 1.0 \times 10^{-16} T_o^{5/2}$$

in c.g.s. units; T is temperature (degrees Kelvin) and the Coulomb logarithm is taken to be 22.

The heat conduction flux is carried mainly by the electrons. If the electrons are magnetized, the volumetric heating rate due to heat conduction is (Braginskii, 1965, p.303)

$$Q_{ther} = \kappa_{\parallel,e} \left(\frac{\partial \delta T}{\partial z}\right)^2 T_o^{-1} \tag{40}$$

where $\kappa_{\parallel,e}$ is the electron heat conductivity along $\underset{\sim}{B}_o$. From Braginskii's equations (2.12) and (2.5e) we have

$$\kappa_{\parallel,e} = 8.4 \times 10^{-7} T_o^{5/2} \tag{41}$$

in c.g.s. units; the Coulomb logarithm is again taken to be 22. If the wave

frequency is very small, then the waves induce nearly adiabatic compressions in the plasma, and we have

$$|\delta T| = (\gamma-1) \, T_o \omega^{-1} |\nabla \cdot \delta \underline{v}| \tag{42a}$$

and equation (40) becomes

$$Q_{ther} = \kappa_{\parallel,e} \, \left(\frac{k_z}{\omega}\right)^2 T_o (\gamma-1)^2 \, (\nabla \cdot \delta v)^2 \tag{42b}$$

(γ is the usual ratio of specific heats, which we shall take to be 5/3). On the other hand, heat conduction can smear out the temperature fluctuations of higher-:requency waves. In the limit of very high frequency, one has

$$|\delta T| = n_o K T_o k_z^{-2} \kappa_{\parallel,e}^{-1} \, |\nabla \cdot \delta \underline{v}| \tag{43a}$$

and

$$Q_{ther} = n_o^{\,2} K^2 T_o k_z^{-2} \kappa_{\parallel,e}^{-1} \, (\nabla \cdot \delta \underline{v})^2 \tag{43b}$$

where K is Boltzmann's constant. At intermediate frequencies neither (42) nor (43) is applicable. We will not do the calculation at this level of detail, however. Instead, we shall use equations (42) if $\omega < \omega_{cond}$, and equations (43) if $\omega > \omega_{cond}$, where ω_{cond} is the angular frequency at which (42b) and (43b) are equal, i.e.

$$\omega_{cond} = \frac{\kappa_{\parallel,e} k_z^2 (\gamma-1)}{n_o K}$$

Finally, we assume that the plasma is optically thin, and radiates Λn^2 erg cm^{-3}s^{-1}, where n is the electron number density and Λ is a tempera-ture-dependent factor which we shall take to be 10^{-22}erg cm^3 s^{-1} at coronal

temperatures (e.g. Rosner, Tucker and Vaiana, 1978, Figure 10). For the purposes of this analysis, we consider only the radiation induced by the waves. The volumetric rate at which radiation extracts energy from the waves is given by

$$Q_{rad} = \Lambda (\delta n)^2 \tag{44a}$$

But mass conservation implies

$$|\delta n| = \frac{n_o |\nabla \cdot \delta \underline{v}|}{\omega} \tag{44b}$$

and thus

$$Q_{rad} = \Lambda n_o^2 \omega^{-2} (\nabla \cdot \delta \underline{v})^2 \tag{44c}$$

Equations (39), (42b) or (43b), and (44c) are the desired expressions for the volumetric rates at which the waves lose energy to the plasma and radiation field. To evaluate these expressions we need to know $\nabla \cdot \delta \underline{v}$. From equations (5)-(8) we obtain

$$\nabla \cdot \delta \underline{v} = - (\varepsilon/B_o^2) k_y^{-1} \delta V_{ky} \cos(k_y y) \exp(ik_z z - i\omega t) \tag{45}$$

The next step in the calculation requires knowledge of the Poynting flux carried by the wave. If the wave electric field is given by

$$\delta \underline{E} = - \delta \underline{v} \times \underline{B}_o/c \tag{46}$$

(c is the speed of light) and if $\delta v_z = 0$, then the z-component of the Poynting flux is

$$S_z = \frac{B_{oz}}{4\pi} \delta \underline{v} \cdot \delta \underline{B} \tag{47}$$

But equation (1) gives

$$\delta B_x = - k_z B_{oz} \delta v_x/\omega \tag{48a}$$

and

$$\delta B_y = - k_z B_{oz} \delta v_y/\omega \tag{48b}$$

Inserting (48) into (47) gives

$$S_z = \frac{B_{oz}^2}{4\pi} \frac{k_z}{\omega} (\delta v_x^2 + \delta v_y^2) \tag{49}$$

Equation (49) is the desired result for the Poynting flux; it is easily shown that the time averages of S_x and S_y vanish if the solution has the form of equations (5).

The damping length of the waves is calculated by equating the volumetric heating and radiation rates to the negative of the divergence of the Poynting flux. However, we first average all quantities over time and over the y-coordinate. And, because the waves vary in x, it is necessary to first integrate over the x-coordinate. Thus, if we denote the e-folding distance for the Poynting flux by L_z, we have

$$L_z = \frac{\int_{-\infty}^{\infty} <\bar{S}_z> dx}{\int_{-\infty}^{\infty} <\bar{Q}_{vis} + \bar{Q}_{ther} + \bar{Q}_{rad}> dx} \tag{50}$$

where the overbar denotes the average over time and the angle brackets denote the average over the y-coordinate.

Evaluation of the integrals in (50) is somewhat tedious, and we merely quote the result. For cases I-IV we find

$$L_z = \frac{B_0^6 k_z}{4\pi \omega} \frac{N}{D} \tag{51}$$

For Case I, N and D are

$$
\begin{aligned}
N_I = & |q_1|^{-1}(1 + k_y^2/q_1^2) \ \sinh^2|q_2|a \\
& + (\sinh 2|q_2|a - 2s|q_2|a)/(2|q_2|) \\
& + k_y^2(\sinh 2|q_2|a + 2s|q_2|a)/(2|q_2|^3)
\end{aligned}
\tag{52}
$$

$$
\begin{aligned}
D_I = & \epsilon_2^2 d_2 \ (\sinh 2|q_2|a + 2s|q_2|a)/(2|q_2|^3) \\
& + \epsilon_1^2 d_1 \ \sinh^2(|q_2|a)/|q_1|^3
\end{aligned}
\tag{53}
$$

where $s = +1$. If $\omega < \omega_{cond}$, the quantity d is

$$d \equiv \frac{n_0}{3} + \kappa_{\shortparallel,e} (\gamma-1)^2 T_0 (\frac{k_z}{\omega})^2 + \Lambda n_0^2/\omega^2 \tag{54}$$

If $\omega > \omega_{cond}$, k_z/ω is replaced by k_z/ω_{cond} on the right-hand side of (54). The damping length for Case II is given by a similar expression, which we will not write down; it is obtained from (52) and (53) by taking $s = -1$ and by replacing $\sinh^2|q_2|a$ with $\cosh^2|q_2|a$. For Case III we find

$$
\begin{aligned}
N_{III} = & |q_1|^{-1}(1 + k_y^2/q_1^2) \sin^2|q_2|a \\
& + (-u\cdot\sin 2|q_2|a + 2|q_2|a)/(2|q_2|) \\
& + k_y^2(u\cdot\sin 2|q_2|a + 2|q_2|a)/(2|q_2|^3)
\end{aligned}
\tag{55}
$$

$$
\begin{aligned}
D_{III} = & \epsilon_2^2 d_2 \ (u\cdot\sin 2|q_2|a + 2|q_2|a)/(2|q_2|^3) \\
& + \epsilon_1^2 d_1 \ \sin^2(|q_2|a)/|q_1|^3
\end{aligned}
\tag{56}
$$

where $u = +1$. The damping length for Case IV is given by a similar expression;

it is obtained from (55) and (56) by taking $u = -1$ and by replacing $\sin^2|q_2|a$
with $\cos^2|q_2|a$.

The behavior of L_z as a function of wave period is illustrated in Figures
2a-d for Cases I-IV. We have taken $\rho_{01}/\rho_{02} = 0.25$, $k_y a = 1.0$, $B_o = 10$ Gauss,
$a = 10^8$cm, $n_{02} = 5 \times 10^9$cm^{-3}, and $T_{01} = T_{02} = 2 \times 10^6$K. Except perhaps for
the magnetic field strength, these parameters might correspond to a solar active
region or to a dense quiet region. The effect of radiation turns out to be
totally negligible for this choice of parameters, and the damping is almost
entirely due to viscosity and heat conduction.

Figure 2 shows that the damping length tends to become very large for
long wave periods. This is particularly evident in Figure 2a, where it is
seen that $L_z \propto \omega^{-4}$ at the long periods. (This dependence on ω results from
the frequency dependence of the τ_2^2 and ϵ_1^2 factors appearing in equations (53)
and (56). These factors reflect the frequency dependence of the compressive-
ness of the waves, i.e. equation (45): low-frequency surface waves are only
weakly compressive, and thus only weakly dissipative. This fact severely
restricts the ability of surface waves to heat the corona. A survey of para-
meters of interest to the corona has revealed that only waves with periods less
that a few tens of seconds will be able to dissipate their energy before pro-
pagating a few tenths of a solar radius.

By the same token, equation (45) shows that the compressiveness is
strongly reduced if B_o is increased. We can therefore anticipate the result,
to be demonstrated below, that the surface wave damping becomes neglible if
B_o exceeds 10 Gauss or so.

Figures 2c and 2d show that the trapped fast waves do dissipate rapidly.
If fast waves can be generated in the corona, they can heat the corona. But it
must again be recalled that the sun may not generate waves of such high frequency.

How do different choices of parameters affect Figure 2? A survey of parameters in the vicinity of those used in Figure 2 has revealed the following:

1. If only k_y is changed: The curves in Figures 2a and 2b move up roughly in proportion to k_y^{-2}, and to the right roughly in proportion to k_y^{-1}. On the other hand, the curves in Figures 2c and 2d are not strongly modified by changes in k_y, except that smaller values of k_y allow the curves to extend to longer periods and larger values of L_z (and vice-versa for larger values of k_y). Overall, we have found that values of $k_y a$ between about 0.5 and 2 lead to the "best" surface wave dissipation in Cases I and II. For smaller values of $k_y a$ the curves are moved up to very large values of L_z, while for larger values of $k_y a$ the curves are moved to the left to very high frequencies.

2. If only a is changed while k_y and all other quantities are held fixed: Figure 2a is essentially unchanged, while Figure 2b is changed mainly by extending to higher (lower) frequencies if a is increased (decreased). The curves in Figures 2c and 2d move to the right roughly in proportion to a, and at high frequencies they move up roughly in proportion to a^2; the maximum levels reached by the curves in Figures 2c and 2d do not respond strongly to changes in a.

3. Increasing (decreasing) B_o increases (decreases) L_z. For Cases I and II at low frequencies, where $L_z \propto \omega^{-4}$, we find that L_z scales as B_o^7 at a given value of ω. (This result is in part dependent on our being in a parameter regime where equations (42) apply at low frequency, and heat conduction dominates viscosity in equation (54). If $T_o = 2 \times 10^6 K$, heat conduction will dominate viscosity if $\omega/k_z \lesssim 1500$ km s^{-1}.) At high frequencies in Figures 2a-d, we find that $L_z \propto B_o$. This means that the waves dissipate much less efficiently in regions of strong magnetic field, and vice-versa.

The ability of surface waves to collisionally damp and heat the corona will
therefore be limited to weak magnetic fields, as in quiet coronal regions.
Our survey of parameters has revealed that the damping lengths become un-
acceptably large if $B_o \geq 10$ Gauss. Coronal active regions are presumed to
have field strengths well in excess of 10 Gauss, and this mechanism fails
in those regions.

4. We have also investigated the consequences of changing n_{o2} and n_{o1},
while n_{o2}/n_{o1} and all other quantities are held constant: The effects of
changing the density are difficult to categorize in detail. But we have
found that in general denser regions have shorter dissipation lengths, and
are more prone to heating by collisional wave dissipation.

Finally, it is useful to note that in most cases where the wave dissi-
pation is significant, the bulk of the heating occurs in the denser region.
To illustrate this point, we plot in Figures 3a-d the ratio of the integrated
heating rate in region 2 to that in region 1, for Cases I-IV, i.e. we plot
the quantity

$$R \equiv \frac{\int_o^a <\bar{Q}_{vis} + \bar{Q}_{ther}>dx}{\int_a^\infty <\bar{Q}_{vis} + \bar{Q}_{ther}>dx} \qquad (57)$$

vs. wave period. (For Case I, R is formally equivalent to the ratio of the
first term on the right-hand side of (53) to the second term with Λ taken to
be zero in d_2 and d_1. For Case III, R is the ratio of the first to the second
term in (56), and similarly for Cases II and IV.) It is clear from the
Figures that the heating occurs primarily in region 2.

VI Validity.

Equation (39) for the viscous heating rate is valid for a collisional plasma. In the present context, this requires

$$\omega \tau_p < 1 \tag{58}$$

where τ_p is the proton collision time. From Braginskii's equation (2.51) we find

$$\tau_p = 0.75 \ T_p^{3/2} n_p^{-1} \quad s \tag{59}$$

for a Coulomb logarithm of 22 (the subscripts 'p' denote protons).

Similarly, equation (40) for the heating due to heat conduction is valid only if the electron mean-free-path, λ_e, is short enough so that

$$k_z \ \lambda_e < 1 \tag{60}$$

If $\lambda_e = \tau_e \ (KT_e/m_e)^{\frac{1}{2}}$, where K is Boltzmann's constant, m_e the electron mass, and τ_e the electron collision time (Braginskii's equation 2.5e), we have

$$\lambda_e = 4.9 \times 10^3 \ T_e^2 \ n_e^{-1} \quad cm \tag{61}$$

Figure 3 shows that the dissipation occurs mainly in region 2, and we therefore evaluate (58)-(61) in that region. We also note that (60-(61) will be more important at lower frequencies, where the heat conduction dominates the viscosity, while (58)-(59) will be more important at higher frequencies, where viscosity dominates heat conduction.

Overall, (58)-(59) turns out to be the most relevant constraints for parameters in the vicinity of those used in Figures 2 and 3. They restrict the validity of our calculations to wave periods greater than 3 seconds or so. The left-most portions of Figures 2 and 3 should therefore be disregarded.

VII. Discussion

Wave theories of coronal heating face the dual challenge of identifying a wave mode which is simultaneously able to propagate the required energy flux into the corona, and to dissipate that energy there. Hollweg (1981a) has suggested that MHD surface waves can in principle satisfy these requirements. Their propagation is similar to that of Alfven waves, which appear capable of propagating energy into the corona (Hollweg, 1981b). And they are compressive even in linearized theory, and therefore capable of heating the plasma via ordinary viscosity and heat conduction.

In the preceding Sections we have discussed coronal surface waves with the intent of assessing whether they can in fact dissipate rapidly enough to heat the corona. We have considered only planar geometries and two cases: a single discontinuity separating two regions of different density, and two parallel discontinuities which enclose a denser region. (The case of two parallel discontinuities admits solutions which are really trapped fast waves, rather than surface waves. We have included these trapped fast wave solutions for completeness.) We have assumed that the discontinuities are structureless, so that resonance absorption need not be considered. And we have assumed that the magnetic pressure dominates the thermal pressure, so that the wave dynamics can be approximately calculated by assuming the plasma to be cold. (Some of our numerical examples have stretched this latter assumption somewhat. For example, the parameters in Figures 2 and 3 imply that the total (electron plus proton) thermal pressure is two thirds of the magnetic pressure.)

We have carried out the analysis under the assumption that the wave periods are long enough for the plasma to be collision-dominated. For the

parameters of interest, this restricts the analysis to wave periods longer
than a few seconds. We have also only approximated the functional behavior
of the temperature fluctuations in the presence of heat conduction. Our
approximation is good in the high and low frequency limits, but we believe
it to be generally adequate for the present purposes.

We have found that the surface wave dissipation lengths are smaller
than a few tenths of a solar radius only if the wave periods are less than
a few tens of seconds. Longer period surface waves have very long damping
lengths, and the waves are then not suitable for coronal heating. The trapped
fast waves can have short damping lengths, of the order of 10^9cm or less, and
they can heat the corona. But the trapped fast waves exist only for short
wave periods, 10 seconds or less in our example, and it is not clear if the
sun generates such waves.

The requirement of such high-frequency waves is a fundamental difficulty.
There is no evidence that the convection zone generates motions with such
hi$_g$h frequencies. Even if motions in the required frequency range were
generated by the convection zone, they would probably dissipate in the photo-
sphere and chromosphere, and not penetrate into the corona as high-frequency
waves. On the other hand, Brueckner (1980) has reported observations of rapid
changes in the chromosphere-corona transition region, occurring on time scales
shorter than 20s; but it is not clear whether these motions are waves; they
seem rather to be impulsive in nature. It is also possible that high-fre-
quency waves can be excited on coronal loops, by the resonances pointed out
by Hollweg (1981b), Ionson (1982), and Zugzda and Locans (1982); as yet there
is no observational evidence that these resonances are excited.

Another difficulty with this mechanism is its extreme sensitivity to
the magnetic field strength. Increasing B_0 slightly can drastically increase
L_z for the surface waves. And increasing B_0 means that the trapped fast waves
can exist only at even higher frequencies, which makes their presence in the
corona even less likely. On the whole, we find that the waves considered in
this paper do not dissipate effectively if $B_0 \gtrsim 10$ Gauss. Larger field
strengths are presumed to exist in active region loops, and the mechanism
investigated here fails in those regions.

Unless the sun generates coronal surface waves with periods shorter than
a few tens of seconds, we conclude that the collisional dissipation of surface
waves is not an effective means of heating the corona, contrary to the suggestion
of Hollweg (1981a).

References

Alfvén, H. 1947, Mon. Not. R. Astron. Soc., 107, 211.

Athay, R. G., and White, O.R. 1979, Ap. J. Suppl., 39, 333.

Braginskii, S.I. 1965, in Reviews of Plasma Physics, 1, 205.

Brueckner, G. E. 1980, in Highlights of Astronomy, 5, 557.

Bruner, E.C., and Poletto, G. 1981, Bull. Am. Astron. Soc., 13, 835.

Bruner, E.C. 1978, Ap. J., 226, 1140.

Burlaga, L.F. 1971, Space Sci. Rev., 12, 600.

Chin, C., and Wentzel, D.G. 1972, Appl. Space Sci., 16, 465.

Chiuderi, C. 1979, in Highlights of Astronomy, 5, 335.

Edwin, P.M., and Roberts, B. 1982, Sol. Phys., 76, 239.

Habbal, S.R., Leer, E., and Holzer, T.E. 1979, Sol. Phys., 64, 287.

Hollweg, J.V. 1978, Geophys. Res. Lett., 5, 731.

Hollweg, J.V. 1981a, Solar Active Regions, ed. Frank Q. Orrall, Colorado
    Associated University Press, p. 277.

Hollweg, J.V. 1981b, Sol. Phys., 70, 25.

Hollweg, J.V. 1982a, Ap. J., 254, 806.

Hollweg, J.V. 1982b, J. Geophys. Res., (submitted).

Hollweg, J.V., Jackson, S., and Galloway, D.J. 1982, Sol. Phys., 75, 35.

Ionson, J.A. 1978, Ap. J., 226, 650.

Ionson, J. A. 1982, Ap. J., 254, 318.

Kuperus, M., Ionson, J.A., and Spicer, D.S. 1981, in Annual Review of
    Astronomy and Astrophysics, 19, 7.

Lee, M. A. 1980, Ap. J., 240, 693.

Lee, M. A., Rae, I.C., and Roberts, B. 1982, (in preparation).

Leer, E., Holzer, T.E., and Fla, T. 1982, (preprint).

Leroy, J.L., and Schwartz, R.D. 1982, Astron. Astrophys., (submitted).

Neubauer, F.M., and Barnstorf, H. 1981, in Solar Wind Four, p. 168.

Osterbrock, D.E. 1961, Ap. J., 134, 347.

Piddington, J. H. 1956, Mon. Not. R. Astron. Soc., 116, 314.

Rae, I.C., and Roberts, B. 1982, Geophys. Astrophys. Fluid Dyn., (in press).

Roberts, B. 1981a, Sol. Phys., 69, 27.

Roberts, B. 1981b, Sol. Phys., 69, 39.

Rosner R., Tucker, W.H., and Vaiana, G.S. 1978, Ap. J. 220, 643.

Schwartz, R.D., and Leroy, J.L. 1982, Astron. Astrophys., (submitted).

Thomas, G.B. 1960, Calculus and Analytic Geometry, (Addison-Wesley Publishing Company Inc.).

Uchida, Y., and Kaburaki, O. 1974, Sol. Phys., 35, 951.

Wentzel, D.G. 1979, Ap. J., 227, 319.

Wentzel, D.G. 1981, in The Sun as a Star, ed. Stuart Jordan, NASA SP 450, 331.

Withbroe, G. 1981, The Sun as a Star, ed. Stuart Jordan, NASA SP 450, 321.

Zugzda, Y.D., and Locans, V. 1982, Sol. Phys., 76, 77.

Figure Captions

Fig. 1. The wave dispersion relations, $\omega^2 a^2/v_{A2}^2$ vs. $k_z^2 a^2$, for surface waves (Cases I and II) and trapped fast waves (Cases III and IV). The graphs are for the case of two parallel TD's, with $\rho_{o1}/\rho_{o2} = 0.25$ and $k_y a = 2$.

Fig. 2. The dissipation length, L_z, vs. wave period for surface waves (Cases I and II) and trapped fast waves (Cases III and IV). The graphs are for the case of two parallel TD's. The parameters for all four cases are given in (a). For the surface waves, it is found that $L_z \propto \omega^{-4}$ at periods longer than a few tens of seconds. Surface waves with periods longer than a few tens of seconds can not heat the corona.
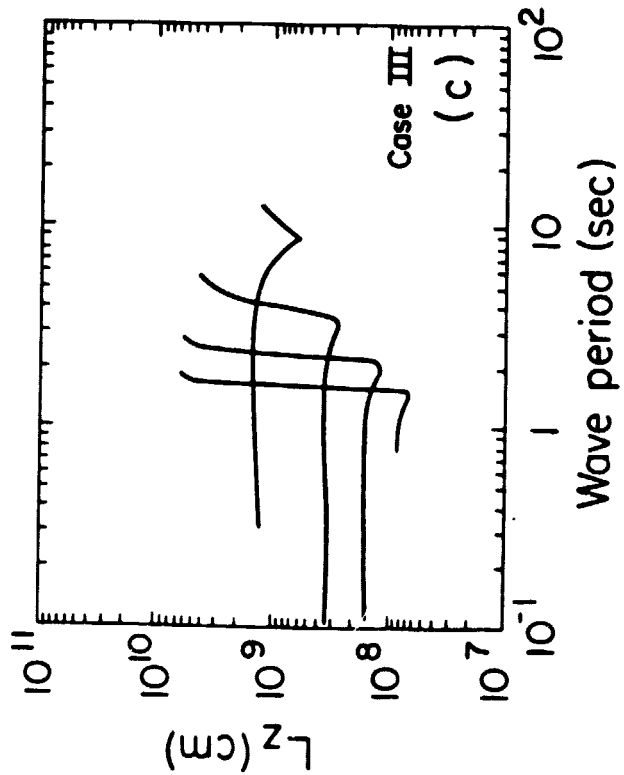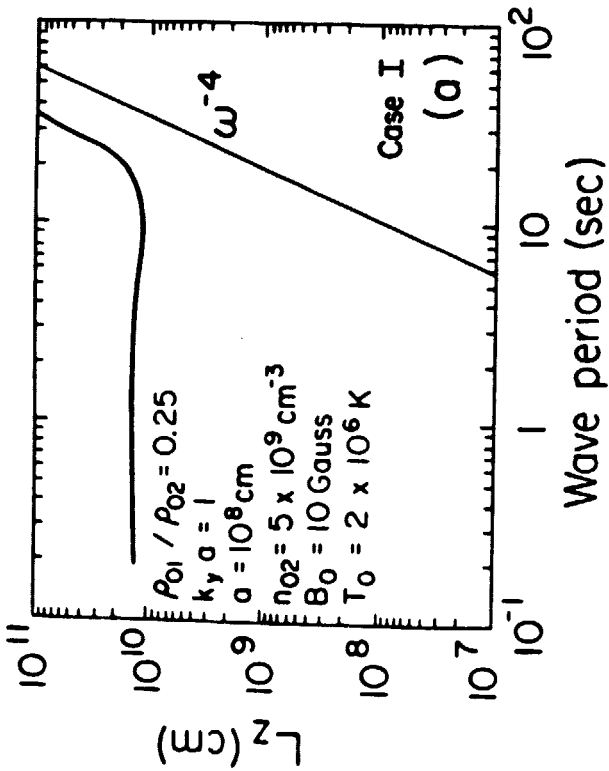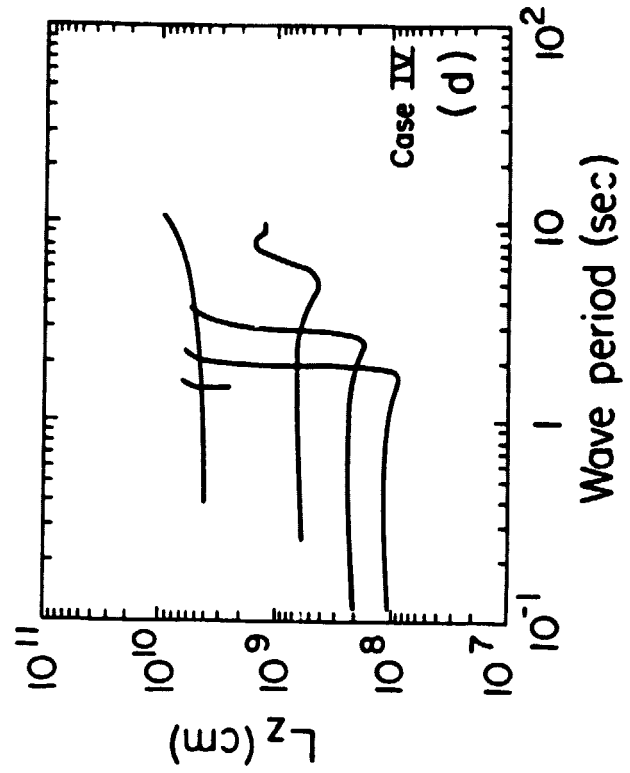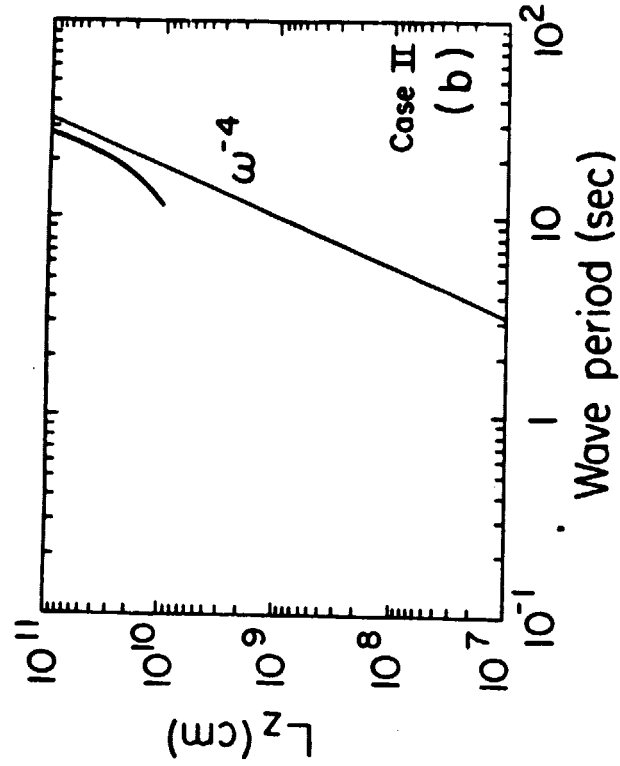
Fig. 3. The ratio of the integrated wave energy loss in region 2 to the integrated energy loss in region 1, for the case of two parallel TD's. All parameters are the same as in Figure 2. There is a strong tendency for most of the wave energy loss to occur in the denser region.

Authors' Mailing address:

        Bruce E. Gordon

        Department of Physics

        University of New Hampshire

        DeMeritt Hall

        Durham, NH 03824 USA

        Dr. Joseph V. Hollweg

        Department of Physics

        University of New Hampshire

        DeMeritt Hall

        Durham, NH 03824 USA

(a) Case I — L_z (cm) vs. Wave period (sec), with ω^{-4} line.

$\rho_{01}/\rho_{02} = 0.25$
$k_y a = 1$
$a = 10^8 cm$
$n_{02} = 5 \times 10^9 cm^{-3}$
$B_0 = 10$ Gauss
$T_0 = 2 \times 10^6 K$

(b) Case II — L_z (cm) vs. Wave period (sec), with ω^{-4} line.

(c) Case III — L_z (cm) vs. Wave period (sec).

(d) Case IV — L_z (cm) vs. Wave period (sec).

Case I (a)

$\rho_{OI}/\rho_{O2} = 0.25$
$k_y a = 1$
$a = 10^8 cm$
$n_{O2} = 5 \times 10^9 cm^{-3}$
$B_0 = 10$ Gauss
$T_0 = 2 \times 10^6 K$

Case II (b)

Case III (c)

Case IV (d)

Wave period (sec)

R